Resource Optimization in Full Duplex Non-orthogonal Multiple Access Systems

Resource Optimization in Full Duplex Non-orthogonal Multiple Access Systems

Keshav Singh, *Member, IEEE*, Kaidi Wang, *Student Member, IEEE*, Sudip Biswas, *Member, IEEE*, Zhiguo Ding, *Senior Member, IEEE*, Faheem Khan, *Member, IEEE*, and Tharmalingam Ratnarajah *Senior Member, IEEE*

***Abstract*—In this paper, we investigate a full duplex (FD) multi-user non-orthogonal multiple access (NoMA) communication system, based on the optimization of received signal-to-interference-plus-noise ratio (SINR) per unit power. Since the communication system operates in FD mode, *co-channel interference (CCI)* and *self-interference (SI)* dominate the system's performance. Accordingly, to combat the CCI, we adopt a game-theoretic approach and propose users clustering algorithms and to suppress the SI, we formulate an optimization problem to maximize the power-normalized SINR (PN-SINR). While the user clustering optimization problem is constrained by i) the successive interference cancellation (SIC) constraint and ii) two binary constraints for the allocations of UL and DL users, the PN-SINR problem is constrained by i) total transmit power budget at the base station and uplink (UL) users, ii) the fundamental condition for the implementation of successive interference cancellation in NoMA, and iii) the minimum fairness condition for UL users. The original PN-SINR problem is non-convex and hence is converted into an equivalent subtractive-form problem, after which we propose an iterative algorithm to find the optimal power allocation policy. Properties of all the proposed algorithms are thoroughly investigated and numerical results are provided. Based on the channel conditions and suppression level of SI and CCI, the superiority of the proposed FD-NoMA system over half duplex NoMA and FD orthogonal multiple access systems is verified.**

***Index Terms*—Non-orthogonal multiple access, full duplex, power allocation, power-normalized SINR, optimization.**

I. Introduction

The explosive growth of mobile users and the advent of Internet-of-Things (IoT) communications in recent years have led to the inevitable search for very high spectrum and power efficient technologies. *Full duplex* (FD) [1]–[4] and *non-orthogonal multiple access* (NoMA) [5]–[10] have emerged as promising technologies to provide higher spectrum efficiency (SE) in 5G and beyond wireless communications systems. In particular, FD communications allows the radios to simultaneously transmit and receive on the same frequency channel, potentially doubling the SE [11]–[14]. Similarly, for the case of NoMA, unlike conventional orthogonal multiple access (OMA), multiple users are served on the same time-frequency resources by exploiting power domain multiplexing to improve the system's SE and achieve higher cell-edge throughput, and low transmission latency [15]–[17]. Thus, both FD and NoMA have been topics of immense interest for a while now and are being investigated extensively.

While both FD and NoMA have been studied separately, to the best of the authors' knowledge, simultaneous NoMA uplink (UL) and downlink (DL) transmission, which can be realized through FD has not been properly investigated yet, both from theoretic, as well as an optimization point of view. One practical scenario where FD-NoMA transmission can assist the communication is when a particular group of DL (or UL) users have poor channel conditions. In such scenarios, the use of FD avoids the spectrum to be solely occupied by these users. However, one of the primary bottlenecks of FD-NoMA or FD in particular is the *strong self-interference (SI)* that arises due to the reception of signals from its own transmitter and the *co-channel interference (CCI)* at the DL users caused by the UL transmission [3]. Though recent research works reveal several techniques to mitigate the strong SI, still some residual SI (RSI) remains, which require further investigation. Further, with regards to the CCI, while works such as [18] consider that the CCI channels between UL and DL users are sufficiently weak, [11] considers a CCI attenuation factor that is assumed to be implemented in prior. Hence, further investigation on the modelling and cancellation of CCI channels is mandatory for the successfull implementation of FD systems. Next, with regards to NoMA, until now it has mostly been explored for enhancing the SE [5]–[10], [19], [20] without considering how the transmit power can be efficiently utilized to acquire such enhancements in SE. Therefore, due to the increasing gap between battery capacity and power consumption of signal processing circuits, energy efficiency (EE) has been considered as a natural performance metric [21]. However, one bottleneck of the EE metric is that it severely constrains the system's performance in low signal-to-noise (SNR) regime [22]–[25]. Consequently, a new metric in the form of power-normalized signal-to-interference-plus-noise ratio (PN-SINR) or SINR-per-unit-power (i.e., performance per unit power) has emerged to measure the performance efficiency [22]–[25] of systems.

In light of the above discussion, this paper, we consider a FD NoMA communication system, where a FD base station (BS) serves multiple UL and DL users simultaneously at the

This work was supported by the U.K. Engineering and Physical Sciences Research Council (EPSRC) under Grant EPSRC-EP/P009549/1. The work of Z. Ding was supported by the UK EPSRC under grant number EP/L025272/2 and by H2020-MSCA-RISE-2015 under grant number 690750.

Keshav Singh, Sudip Biswas, and Tharmalingam Ratnarajah are with Institute for Digital Communications, School of Engineering, University of Edinburgh, Edinburgh, UK. (E-mail: {k.singh, sudip.biswas, t.ratnarajah}@ed.ac.uk)

Kaidi Wang and Zhiguo Ding are with School of Electrical and Electronic Engineering, University of Manchester, Manchester, UK. (E-mail: kaidi.wang@postgrad.manchester.ac.uk, zhiguo.ding@manchester.ac.uk)

Faheem Khan is with School of Computing and Engineering, University of Huddersfield, Queensgate, Huddersfield, UK. (Email: f.khan@hud.ac.uk)

The corresponding author of this paper is Sudip Biswas.

same time and frequency resources. It is assumed that all the UL and DL users are equipped with single antenna, while the BS has two antennas, one each for reception and transmission. To mitigate the CCI, we perform smart channel assignments by formulating a user clustering optimization problem, subject to successive interference cancellation (SIC) constraint and two binary constraints for the allocations of UL and DL users. Next, we formulate a power allocation optimization problem for controlling the RSI under the constraints of the total transmit power budget at the BS and UL users, the fundamental condition for the implementation of SIC in DL NoMA, and the minimum fairness condition for UL users. The main contributions of this paper are summarized as follows:

- Since the formulated clustering problem for UL and DL users is non-convex and it is very difficult to solve, we propose a game-theoretic approach [26] to find the optimal clustering for UL and DL users. In addition, we analyse several properties of the proposed user clustering algorithms such as complexity, convergence behavior, and the stability of the algorithms.
- By exploiting the properties of fractional programming [27], we transform the original PN-SINR fractional problem into an equivalent subtractive-form problem and then perform dual-layer optimization. Next, we propose an iterative algorithm to find the optimal power allocation policy.
- Finally, we evaluate the performance of the proposed algorithms for the FD NoMA system through rigorous computer simulations. Numerical results demonstrate the superiority of FD NoMA over HD NoMA, and FD OMA systems.

A. Paper organization

The rest of the paper is organized as follows. In Section II, we introduce the system model for the FD NoMA communication system and illustrate some of the preliminaries required for the analysis. The hybrid NoMA scheme, power consumption model, and the efficiency measure, PN-SINR are described in Section III. The formulation of the optimization problems for user clustering and the power allocation and the proposed algorithms are provided in Section IV. Numerical results are provided in Section V, followed by concluding remarks in Section VI.

B. Notation

The following notations are used throughout the paper. $\mathbb{E}[X]$ denotes the expected value of the random variable X, $X \sim \mathcal{CN}(\mu, \sigma^2)$ denotes a circularly symmetric complex Gaussian random variable X with mean μ and variance σ^2 and $|\cdot|$ denotes the absolute value of a complex valued scalar. Any other notations will be explicitly defined wherever used.

II. System Model

We consider a NoMA communication system as shown in Fig. 1, where a FD BS serves K single antenna UL and J DL users at the same time and frequency resource. The

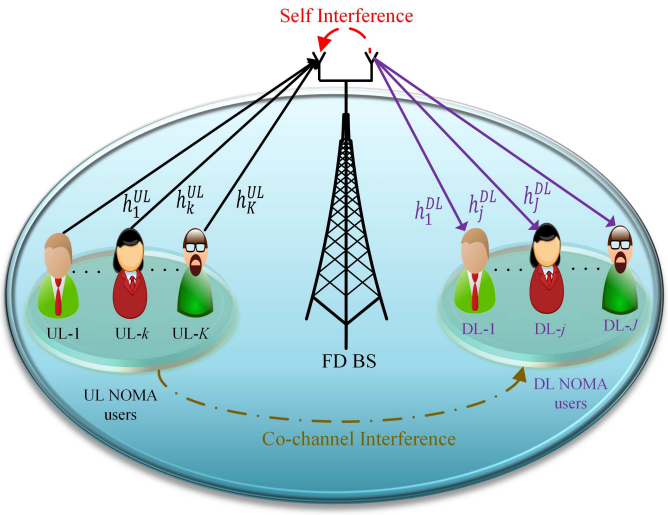

Fig. 1: An illustration of the considered multi-user FD NoMA communication system. The FD system suffers from RSI and CCI.

BS is equipped with two antennas, one each for reception and transmission. Further, hardware impairment is a plausible predicament in FD systems[1]. Accordingly, in this work we consider the limited dynamic range of hardwares, which is described in the following subsection.

A. Hardware Impairment Model

In particular, to model the inherent imperfection of the transmit and receive chains, we adopt the transmitter/receiver distortion model in [3], which accounts for the non-ideal hardware components, e.g., digital-to-analog converters (DACs), analog-to-digital converters (ADCs), amplifiers, oscillators, etc. The aforesaid model has been shown to be valid through experimental measurements in [28] and [29]. It was stated that the cumulative effects of hardware imperfections can be reasonably approximated as an additive Gaussian noise. In conjunction to several other literature [11], [12], which also use the same hardware impairment model, we consider an additive white Gaussian term as "transmitter noise" ("receiver distortion") at each transmit (receive) antenna, whose variance is κ (β) times the power of the undistorted signal at the corresponding chain. Global CSI is assumed to be available at the BS and users. In the following we describe the proposed FD MIMO-NoMA framework. Since we consider the BS to operate in FD mode, it suffers from SI and CCI.

B. DL and UL Communication

Let P_{BS} denotes the total transmission power of the BS, P_{D_j} be the power allocation coefficient for the jth DL user and s_j^{DL} be the transmitted source symbol intended for the jth DL user such that $\mathbb{E}\left[|s_j|^2\right] = 1$, $\forall j \in \{1, \ldots, J\}$. Note that

[1]Compared to HD systems, the impact of hardware impairments is severe in FD systems due to the strong SI, see, e.g., specifications of SI cancellation for 802.11ac PHY [2]. This is due to the fact that while the distortions originating from the transmit chains pass through a strong SI channel and become significant, on the receiver chains they are more prone to distortion due to the high-power received signal.

the signals transmitted and received by the BS are denoted by $\tilde{y}_0$ and y_0, respectively, while the superscripts UL and DL are used only for the signals transmitted by UL users and received by DL users, respectively. Then, the transmitted signal by the BS is given as

$$\tilde{y}_0 = \sum\nolimits_{j=1}^{J} \sqrt{P_{D_j}} s_j. \tag{1}$$

In the above, $\tilde{y}_0$ denotes the superposition of s_j symbols with power allocation policy $\mathcal{P}_D = \left\{[P_{D_1}, P_{D_2}, \ldots, P_{D_J}] | \sum_{j=1}^{J} P_{D_j} = P_{BS}\right\}$.

Similarly, let P_{U_k} be the transmit power of the kth UL user with $\mathcal{P}_U = \{P_{U_1}, P_{U_2}, \ldots, P_{U_K}\}$ being the set of transmit powers of K UL users, s_k^{UL} be the transmitted source symbol of the kth UL user such that $\mathbb{E}\left[|s_k|^2\right] = 1, \forall k \in \{1, \ldots, K\}$. Then, the transmitted signal by the UL k is given as

$$\tilde{y}_k^{UL} = \sqrt{P_{U_k}} s_k. \tag{2}$$

Now, the signal received by the jth DL user can be given as

$$y_j^{DL} = \underbrace{h_j^{DL}(\tilde{y}_0 + c_0)}_{\text{Desired signal + intra-user interference + transmitter distortion}} + \underbrace{\sum_{k=1}^{K} h_{jk}^{DU}(\tilde{y}_k^{UL} + c_k^{UL})}_{\text{CCI}} + \underbrace{e_j^{DL} + n_j^{DL}}_{\text{Receiver distortion + noise}}. \tag{3}$$

Similarly, the signal received by the BS from K UL users can be given as

$$y_0 = \underbrace{\sum\nolimits_{k=1}^{K} h_k^{UL}(\tilde{y}_k^{UL} + c_k^{UL})}_{\text{Desired signal + intra-user interference + transmitter distortion}} + \underbrace{h_0(\tilde{y}_0 + c_0)}_{\text{SI}} + \underbrace{e_0 + n_0}_{\text{Receiver distortion + noise}}. \tag{4}$$

In the above, h_j^{DL}, h_k^{UL}, h_0, and h_{jk}^{DU} denote the DL channel of the jth DL user, UL channel of the kth UL user, RSI channel, and the CCI channel between the kth UL and jth DL users, respectively, and n_j^{DL} and n_0 denote the noise for DL and UL cases with variances σ_0^2 and σ_j^2, respectively. Further, in (3) and (4), c_k^{UL} (c_0) is the distortion at the transmitter at the kth UL user (BS), which closely approximates the effects of phase noise, non-linearities in the DAC and additive power-amplifier noise. The variance of c_k^{UL} and c_0 is given by κ ($\kappa \ll 1$) times the transmit power of the signal at each antenna [3]. These distortions are statistically independent from the transmitted signals, and can be modeled as c_k^{UL} and c_0 as [12]

$$\begin{aligned} c_k^{UL} &\sim \mathcal{CN}\left(0, \kappa P_{U_k}\right), \\ c_0 &\sim \mathcal{CN}\left(0, \kappa \sum\nolimits_{j=1}^{J} P_{D_j}\right). \end{aligned} \tag{5}$$

Similarly, e_j^{DL} (e_0) is the receiver distortion at the jth DL user (BS), which closely approximates the combined effects of non-linearities in the ADC, additive gain-control noise and phase noise. The variance of e_j^{DL} is given by β ($\beta \ll 1$) times the power of the undistorted received signal at each receive antenna [3]. The receiver distortions are also statistically independent from the received signals and accordingly, e_j^{DL} and e_0 can be modeled as [12]

$$\begin{aligned} e_j^{DL} &\sim \mathcal{CN}\left(0, \beta \text{var}\left(y_j^{DL} - e_j^{DL}\right)\right), \\ e_0 &\sim \mathcal{CN}\left(0, \beta \text{var}\left(y_0 - e_0\right)\right). \end{aligned} \tag{6}$$

Since the BS knows the interfering codewords $\tilde{y}_0$ and its SI channel $h_0\tilde{y}_0$, so the SI term is known, and thus can be cancelled [3]. The channel state information (CSI) of the SI channel can be acquired by using pilot signals. Since the pilot signal of a FD node is echoed back to itself, and the received power of this echoed-backed pilot signal is very high (due to small distances between transmit and receive antennas of a node), the SI channel can be estimated with high accuracy [30]. Accordingly, the SI cancelled signal can be written as

$$\begin{aligned} \bar{y}_0 &= y_0 - h_0\tilde{y}_0 \\ &= \sum\nolimits_{k=1}^{K} h_k^{UL}(\tilde{y}_k^{UL} + c_k^{UL}) + \underbrace{h_0 c_0}_{\text{RSI}} + e_0 + n_0. \end{aligned} \tag{7}$$

In the above $h_0 c_0$ is the residual SI (RSI) which remains, due to the fact that in practice, even if the SI is suppressed to some extent using analog and digital SI cancellation techniques, due to transmitter and receiver distortions, the SI may not be cancelled completely resulting in RSI.

C. Remarks

1) RSI as Hardware Impairments: It is worth noting that the values of the distortion coefficients κ and β relate the undistorted receive and transmit signal variance to the variance of the corresponding distortion. Hence, κ and β reflect the amount of RSI left in the system. In other words, the higher the values of κ and β, higher is the RSI. Hereinafter, κ and β will be called upon as RSI mitigation (RSIM) coefficient.

2) CSI Estimation: In this work we assume that the BS knows the users' channel state information (CSI) perfectly as in [19],[31]–[33]. This is performed via the exchange of training sequences and feedback, and the application of usual CSI estimation methods [34]. Note that the acquisition of perfect CSI may not be feasible and effective estimation methods can be found in existing FD literature [35]. Further, it has been proved that the impact of CSI error is negligible for scenarios where a sufficiently long training sequence is employed. Therefore, the considered framework works best for scenarios with block flat-fading channels, where the channels are static within a particular time-frequency coherence block and long training sequences can be utilized. For scenarios where the CSI can not be accurately obtained, the results of this paper can be treated as theoretical guidelines (possible upper bounds) on the effects of RSI and CCI in a NoMA FD system, if CSI were accurately known.

3) User Ordering: Since NoMA transmission is employed, user ordering plays an important role in successful implementation of the framework. Several techniques for user ordering have been proposed in literature [7]-[8] and hence, finding the optimal ordering is not the focus of this paper. We assume that there exists a method to solve the ordering problem and

we are provided with ordered users. Accordingly this work focusses on resource optimization, that maximizes the SE and EE of the system, for a given user ordering.

4) CCI Mitigation: Since the FD BS serves K UL and J DL users at the same time and frequency resource, DL users have to encounter additional CCI from UL transmission. However, the CCI is usually controlled via scheduling [36] or assuming the channels between UL and DL users to be sufficiently weak [18]. However, in this work we mitigate the CCI through smart channel assignments, which is done with the help of Game Theory by clustering the UL and DL users at a stage prior to the power allocation phase. Note that the users with sufficiently weak CCI channels are clustered together through Algorithm 1 and 2, after which NoMA is applied in each cluster for communications. Hence, the CCI channels between UL and DL users do not have impact on the decoding order for NoMA communications.

III. Hybrid NoMA Scheme

For allocating the UL and DL users, T resource blocks are introduced and the users allocated into the same resource block are considered as a cluster. Different bandwidth resources (time/frequency) can be employed, where the channel coefficients are unchanged among these resource blocks. The collections of all DL and UL users are denoted by $\mathcal{J} = \{1, 2, \ldots, J\}$ and $\mathcal{K} = \{1, 2, \ldots, K\}$, respectively, while $\mathcal{S} = \{S_1, \ldots, S_T\}$ denotes the collection of all clusters. We consider a hybrid multiplexing scheme, where NoMA is employed in each cluster, and the users of different clusters receive signals via OMA schemes.

A. DL Communication

In any cluster S_t with $\widetilde{J}$ DL users and $\widetilde{K}$ UL users, the jth DL user can receive its signal with the SINR given in (8), as shown on the top of the next page, where $\Psi_j^{DL} = \sum_{j=1}^{\widetilde{J}} P_{D_{t,j}} |h_{t,j}^{DL}|^2 + \sum_{k=1}^{\widetilde{K}} P_{U_{t,k}} |h_{t,jk}^{DU}|^2$, $P_{D_{t,j}}$ denotes the transmission power for the jth DL user in S_t cluster, $h_{t,j}^{DL}$ and $h_{t,jk}^{DU}$ indicate the DL channel of the jth DL user in S_t cluster and the CCI channel between the kth UL and jth DL users in S_t cluster, respectively, and σ_j^2 denotes the noise variance for the jth DL user.

By considering the indicator of each user, the individual SINR of the jth user in cluster S_t can be expressed as follows:

$$\widetilde{\gamma}_{t,j}^{DL} = x_{t,j}^{DL} \omega_t \gamma_{t,j}^{DL}, \tag{9}$$

where $x_{t,j}^{DL}$ is the indicator of user j and cluster S_t, and ω_t^{DL} is the resource allocation coefficient of cluster S_t. More particularly, $x_{t,j}^{DL} = 1$ implies that the DL user j is allocated into cluster S_t; $x_{t,j}^{DL} = 0$ otherwise. Additionally, the resource allocation coefficients satisfy $\sum_{t=1}^{T} \omega_t = 1$. The total SINR for DL users for the hybrid NoMA system is

$$\Gamma^{DL} = \sum\nolimits_{t=1}^{T} \sum\nolimits_{j=1}^{\widetilde{J}} x_{t,j}^{DL} \omega_t \gamma_{t,j}^{DL}. \tag{10}$$

Remark 1: The bandwidth resources (time/frequency) can be equally allocated to all clusters, i.e., $\omega_t = \frac{1}{T}, \forall S_t \in \mathcal{S}$. Note that it is possible to use different resource allocations at different clusters. Resource allocation with such a different consideration is an important direction for future research, but it is out of the scope of this paper.

B. Uplink Communication

The SINR for the kth UL user in cluster S_t can be given by (11), as shown on the top of the next page, where $h_{t,k}^{UL}$ and h_0 represent the UL channel of the kth UL user in S_t cluster and RSI channel, respectively. Here, σ_0^2 denotes the noise variance at the BS.

Similar to (10), the total SINR for UL users for the hybrid NoMA system is

$$\Gamma^{UL} = \sum\nolimits_{t=1}^{T} \sum\nolimits_{k=1}^{\widetilde{K}} x_{t,k}^{UL} \omega_t \gamma_{t,k}^{UL}, \tag{12}$$

where $x_{t,k}^{UL}$ is the connection indicator of user k and resource block t.

C. Power Consumption Model

To achieve the above SINR the total required power for the system can be given as

$$\mathcal{P}_T = \underbrace{P_{BS}}_{\text{Total transmit power for DL}} + \underbrace{P_U}_{\text{Total transmit power for UL}} + \underbrace{P_{CP}}_{\text{Circuit power consumption}}, \tag{13}$$

where $P_{BS} = \sum_{t=1}^{T} \sum_{j=1}^{\widetilde{J}} P_{D_{t,j}}$, $P_U = \sum_{t=1}^{T} \sum_{k=1}^{\widetilde{K}} P_{U_{t,k}}$ and P_{CP} refers to the circuit power consumption in the system. While P_{CP} is considered to be fixed in most works [11] for simplicity, it may not be a true representation of the power consumption both at the BS as well as the users. Accordingly, in this paper we consider a circuit power consumption model that accounts for the number of users in the system as well as the maximum achievable sum rate.

1) Pragmatic Circuit Power Consumption Model: The circuit power consumption P_{CP} in the system is the resultant of the total power consumed by various digital signal processing blocks and analog components. In conjunction to [37], [38], in this work we consider the following circuit power consumption model.

$$P_{CP} = P_{Fix} + P_{RF} + P_{LO}. \tag{14}$$

Each term of the right hand side of (14) is explained below.

a) Fixed Power: P_{Fix} refers to the fixed power necessary for air conditioners, control signalling, load independent power of backhaul processing, etc.

b) Radio Frequency Chains: P_{RF} is the power consumed by the circuit components of the transmitters and receivers of the system, such as ADCs, DACs, mixers, filters, etc., attached to each antenna at the BS and each individual user. Accordingly, it is given as

$$P_{RF} = 2P_{BS}^{C} + KP_{U}^{C}, \tag{15}$$

where P_{BS}^{C} and P_{U}^{C} are the power required by all circuit components at the BS per antenna and each user.

$$\gamma_{t,j}^{DL} = \frac{P_{D_{t,j}}|h_{t,j}^{DL}|^2}{\sum_{i=j+1}^{\widetilde{J}} P_{D_{t,i}}|h_{t,j}^{DL}|^2 + \kappa\sum_{i=1,i\neq j}^{\widetilde{J}} P_{D_{t,i}}|h_{t,j}^{DL}|^2 + (1+\kappa)\sum_{k=1}^{\widetilde{K}} P_{U_{t,k}}|h_{t,jk}^{DU}|^2 + \beta\Psi_j^{DL} + \sigma_j^2}, \tag{8}$$

$$\gamma_{t,k}^{UL} = \frac{P_{U_{t,k}}|h_{t,k}^{UL}|^2}{\sum_{i=1,i>k}^{\widetilde{K}} P_{U_{t,i}}|h_{t,i}^{UL}|^2 + \kappa\sum_{i=1}^{\widetilde{K}} P_{U_{t,i}}|h_{t,i}^{UL}|^2 + \kappa\sum_{j=1}^{\widetilde{J}} P_{D_{t,j}}|h_0|^2 + \beta\sum_{i=1}^{\widetilde{K}} P_{U_{t,i}}|h_{t,i}^{UL}|^2 + \sigma_0^2}, \tag{11}$$

c) Local Oscillator : P_{LO} is the power consumed by the local oscillator at each transmit node for frequency synthesis and is given as

$$P_{LO} = P_{LO_{BS}} + KP_{LO_U}. \tag{16}$$

D. Power-Normalized SINR

The PN-SINR of a communication system as described in Section I can be defined as the ratio between the total SINR and the total power consumed. Accordingly, it can be mathematically given as

$$\eta = \frac{\Gamma^{DL} + \Gamma^{UL}}{\mathcal{P}_T}. \tag{17}$$

IV. Problem Formulation and Proposed Algorithms

In this section, firstly, we will propose two algorithms based on a *game theoretic approach* for user selection and clustering for DL and UL users. Further, the properties of both algorithms will be illustrated. Secondly, a power allocation algorithm will be investigated. In this work NoMA principle is used for transmission. For the DL, NoMA employs successive interference cancellation (SIC) at individual DL user based on a particular ordering. Similarly, for the UL, channels for each individual user can be ordered and the BS can employ SIC for each UL user's channel.

From Fig. 1, let us consider that the 1st user is the weakest (and hence cannot decode any interfering signals), and $\widetilde{J}$th user is the strongest user in cluster S_t, which is able to attenuate interference from all other users in cluster by performing SIC. The other users are placed in an increasing order with respect to their index numbers. For example, user j is placed before user i if $j < i$. Accordingly, without loss of generality we consider that the effective channel gains between BS and $\widetilde{J}$ DL users for the S_t cluster are ordered as [7], [8]

$$\left|h_{t,1}^{DL}\right|^2 \leq \left|h_{t,2}^{DL}\right|^2 \ldots \leq \left|h_{t,j}^{DL}\right|^2 \leq \left|h_{t,i}^{DL}\right|^2 \ldots \leq \left|h_{t,\widetilde{J}}^{DL}\right|^2. \tag{18}$$

In line with the optimal SIC decoding order, the ith DL user in S_t cluster can successfully decode the message of $j$the DL user for $j \leq i$ and then remove this message from its observed mixture in a successive fashion, with the ith user's message for $i > j$ being regarded as noise by DL user j. For sake of simplicity, let $\sigma_0^2 = \sigma_j^2 = \sigma^2$, $\forall j$. Then, the instantaneous SINR for ith user to detect the message of jth user in S_t cluster for $j \leq i$, is denoted as (19), as shown on the top of the next page. Once the $j \leq i$ messages are decoded successfully, the ith user in the cluster can decode its own message with the SINR given in (8).

A. Problem Formulation: User Clustering

Using (17) and (19), the user clustering problem for maximizing the PN-SINR can be formulated as

$$\begin{aligned}
(\mathbf{P0}) \quad & \max_{\mathcal{X}^{DL},\mathcal{X}^{UL}} \quad \frac{\Gamma^{DL} + \Gamma^{UL}}{\mathcal{P}_T} \\
\text{s.t.} \quad & (C.1) \quad \gamma_{t,i\to t,j}^{DL} \geq \gamma_{t,j}^{DL}, \qquad \forall j < i, j \neq J, \forall S_t \in \mathcal{S}, \\
& (C.2) \quad x_{t,j}^{DL} \in \{0,1\}, \qquad \forall j \in \mathcal{J}, \forall S_t \in \mathcal{S}, \\
& (C.3) \quad x_{t,k}^{UL} \in \{0,1\}, \qquad \forall k \in \mathcal{K}, \forall S_t \in \mathcal{S}, \\
& (C.4) \quad \sum_{t=1}^{T} x_{t,j}^{DL} = 1, \qquad \forall j \in \mathcal{J}, \\
& (C.5) \quad \sum_{t=1}^{T} x_{t,k}^{UL} = 1, \qquad \forall k \in \mathcal{K},
\end{aligned} \tag{20}$$

where $\mathcal{X}_{DL}$ and $\mathcal{X}_{UL}$ are the collections of all DL and UL indicators, respectively. More particular, $\mathcal{X}_{DL} = \{\mathbf{x}_1^{DL}, \mathbf{x}_2^{DL}, \cdots, \mathbf{x}_J^{DL}\}^T$ and $\mathcal{X}_{UL} = \{\mathbf{x}_1^{UL}, \mathbf{x}_2^{UL}, \cdots, \mathbf{x}_K^{UL}\}^T$, where $\mathbf{x}_j^{DL} = \{x_{1,k}^{DL}, x_{2,k}^{DL}, \cdots, x_{T,k}^{DL}\}$ and $\mathbf{x}_k^{UL} = \{x_{1,k}^{UL}, x_{2,k}^{UL}, \cdots, x_{T,k}^{UL}\}$. The constraint $(C.1)$ mandates the SIC condition, while the symbol $x_{t,j}^{DL}$ in constraint $(C.2)$ is a binary variable whose value is 1 if jth DL user is allocated in the S_t cluster, and 0 otherwise. Similarly $x_{t,k}^{UL} = 1$ if kth UL user is assigned in S_t cluster, and 0 otherwise. Further, the constraints $(C.4)$ and $(C.5)$ ensure that a DL and UL user can only be allocated into only one cluster at the same time, respectively.

The above problem can be solved by utilizing a *game theoretic approach* [26]. In particular, for a given set of power allocation coefficients, the user clustering problem can be modelled as a distributed user clustering game $(\mathcal{J}, \mathcal{K}, U)$. The coalition utility of any cluster S_t is defined as the sum utility of all users in this cluster as follows:

$$U(S_t) = \frac{\sum_{j=1}^{J} \widetilde{\gamma}_{t,j}^{DL} + \sum_{k=1}^{K} \widetilde{\gamma}_{t,k}^{UL}}{P_T}, \tag{21}$$

where $\widetilde{\gamma}_{t,j}^{DL}$ is given by (8), and $\widetilde{\gamma}_{t,k}^{UL} = x_{t,k}^{UL}\omega_t\gamma_{t,k}^{UL}$. According to [26], the user clustering game $(\mathcal{J}, \mathcal{K}, U)$ is a characteristic formation game with non-transferable utility, since the coalition utility is a mapping function and only depends on the users in the same cluster. In order to resolve the user clustering game, a preference relation based approach is proposed, where the players swap form one cluster to another based on its preference. A notation $\prec$ is introduced for denoting the preference relation of the users. Consider a situation with one user i and two clusters S_t and $S_{t'}$, where $i \in S_t$, $S_t \cap S_{t'} = \emptyset$. Then, $S_t \prec_i S_{t'}$ indicates that user i is willing to be part of cluster $S_{t'}$, rather than cluster S_t. The preference relation is considered as

$$S_t \prec_i S_{t'} \Leftrightarrow U(S_t) + U(S_{t'}) < U(S_t \backslash \{i\}) + U(S_{t'} \cup \{i\}), \tag{22}$$

$$\gamma_{t,i\to j}^{DL}=\frac{P_{D_{t,j}}|h_{t,i}^{DL}|^2}{|h_{t,i}^{DL}|^2\sum_{l=j+1}^{\widetilde{J}}P_{D_{t,l}}+\kappa\sum_{l=1,l\neq i}^{\widetilde{J}}P_{D_{t,l}}|h_{t,i}^{DL}|^2+(1+\kappa)\sum_{k=1}^{\widetilde{K}}P_{U_{t,k}}|h_{t,jk}^{DU}|^2+\beta\Psi_i^{DL}+\sigma^2}. \tag{19}$$

Algorithm 1 User Clustering Algorithm for DL Users (UCA-DL)

Initialization Phase

1: Allocate all DL users into singleton clusters, i.e., $S_j = \{j\}$, where $j \in \mathcal{J}$.
2: Record current structure as $\mathcal{S}$.

User clustering Phase

For any DL user $j \in \mathcal{J}$, where $j \in S_t$, $S_t \in \mathcal{S}$,

1: User j visits all other clusters from S_1 to S_T except its current cluster.
2: For any cluster $S_{t'} \in \mathcal{S}$, where $t' \neq t$.
3: Calculate the sum utilities of clusters S_t and $S_{t'}$.
4: User j moves from cluster S_t to $S_{t'}$, the new user structure $\mathcal{S}_{new}$ is obtained.
5: All users in clusters S_t and $S_{t'}$ are ordered based on the condition of SIC $(C.1)$.
6: Calculate the new sum utilities of clusters S_t and $S_{t'}$.
7: Compare the preference of DL user j based on the strictly preference relation function (22).
8: If the preference relation $S_t \prec_j S_{t'}$ is satisfied, record current structure as $\mathcal{S} = \mathcal{S}_{new}$.
9: Else, switch the user structure back to $\mathcal{S}$.

Algorithm 2 User Clustering Algorithm for UL Users

Initialization Phase

1: Allocate all UL users into cluster S_0.
2: Record current structure as $\mathcal{S}$.

User clustering Phase

For any UL user $k \in \mathcal{K}$, where $k \in S_t$, $S_t \in \mathcal{S} \cup S_0$,

1: User k visits all other clusters in $\mathcal{S}$ except its current cluster.
2: For any cluster $S_{t'} \in \mathcal{S}$, where $t' \neq t$.
3: Calculate the sum utilities of clusters S_t and $S_{t'}$.
4: User k moves from cluster S_t to $S_{t'}$, the new user structure $\mathcal{S}_{new}$ is obtained.
5: Calculate the new sum utilities of clusters S_t and $S_{t'}$.
6: Compare the preference of UL user k based on the strictly preference relation function (22).
7: If the preference relation $S_t \prec_k S_{t'}$ is satisfied, record current structure as $\mathcal{S} = \mathcal{S}_{new}$.
8: Else, switch the user structure back to $\mathcal{S}$.

where $U(S_t)$ is the sum utility of all users in cluster S_t. That is, if user i decides to move from cluster S_t to cluster $S_{t'}$, the sum utilities of clusters S_t and $S_{t'}$ are strictly increased with the swap operation of user i. Each user compares the preference with all other clusters, and swaps to any other cluster if the condition in inequality (22) is satisfied. By introducing the compare-and-swap operation, the *user clustering algorithm for DL users* (UCA-DL) is illustrated in **Algorithm 1**.

After allocating all DL users into the clusters, the *user clustering algorithm for UL users* (UCA-UL) is performed. Note that the UL users are grouped based on the fixed user structure of DL users, since UCA-UL is performed after UCA-DL. Hence, an extra cluster S_0 is introduced for including all UL users in the initialization phase. The proposed algorithm for clustering the UL users is described in **Algorithm 2**.

During UCA-DL and UCA-UL, all DL and UL users are respectively clustered into user structure $\mathcal{S}$. In the user clustering phase, the users perform the compare-and-swap operation from the first user to the last one. For any user, if it has successfully visited all other clusters, its operation is finished and the next user start the compare-and-swap operation. If the last user has finished the user clustering phase, the first user start the game again. Note that the optimal decoding order is not considered in UCA-UL, since the data rate is not effected by the sequence of UL users. The algorithm is completed until no user has the intention to join in another clusters and the final structure is the optimal user structure.

B. Property Analysis of Algorithms

For evaluating the proposed user clustering algorithms, the properties including complexity, convergence, and stability, are analyzed in this subsection. The proposed user clustering algorithms for both DL and UL users are based on the preference relation method, and hence, the properties of these algorithms are considered together.

1) Complexity: Note that the proposed user clustering algorithms are repeated until no users can join in another cluster. Hence, the complexity of the algorithms is related to the number of cycles. With a given number of cycles C, the complexity of the proposed algorithms can be present as follows:

Proposition 1: In UCA-DL and UCA-UL, at most $J(J-1)$ and J^2 times of the computational operations are respectively performed in each cycle. With a given number of cycle times C, the computational complexity of UCA-DL and UCA-UL is approximated as $\mathcal{O}(CJ^2)$.

Proof: In UCA-DL and UCA-UL, the number of the computational times is based on the compare-and-swap operations of the individual user, since there is one time of computations when any user compare the change of the sum utility according to the preference relation (22). Any user needs to perform the compare-and-swap operations for all other clusters. Therefore, the worst case is that all users stay in the singleton clusters. In the worst case, there are J clusters and the DL user in UCA-DL needs to compute the sum utility for $J-1$ times. For the UL users, there are J clusters can be joined, since UCA-UL is performed after UCA-DL and all UL users are staying in cluster S_0 in the initialization phase. In one cycle, all users need to perform the compare-and-swap operations. Hence, the computational complexities of UCA-DL and UCA-UL in one cycle are $J(J-1)$ and J^2, respectively. Given a number of

cycle times C, the computational complexity of UCA-DL and UCA-UL can be expressed as $\mathcal{O}(CJ^2)$. ■

2) Convergence: The convergence of the proposed algorithm 1 and algorithm 2 is present as follows:

Proposition 2: From any initial user structure $\mathcal{S}_{init}$, the user clustering game $(\mathcal{J}, \mathcal{K}, U)$ with UCA-DL and UCA-UL is guaranteed to converge to a final structure $\mathcal{S}_{final}$.

Proof: In UCA-DL and UCA-UL, the users perform the compare-and-swap operations for increasing the sum utility of the system. The operations can be divided into two steps. Firstly, the users calculate the increment of sum utility. Secondly, the users decide to join in another cluster if the increment is positive. The transformation of user structure is only effected by the second step, i.e., the swap operation, since any user is moved to another cluster. During the game, the user structure is transformed as follows:

$$\mathcal{S}_{init} \rightarrow \mathcal{S}_1 \rightarrow \mathcal{S}_2 \rightarrow \cdots \rightarrow \mathcal{S}_{final}. \tag{23}$$

Assume that $\mathcal{S}_a$ and $\mathcal{S}_b$ are two user structures in sequence (23), and $\mathcal{S}_b$ is the next structure of $\mathcal{S}_a$. From $\mathcal{S}_a$ to $\mathcal{S}_b$, there exits one user successfully swapped from one cluster to another one. The swap operation meets the condition in (22), that is, the sum utilities of the two clusters are increased. Recall that the user clustering game is in characteristic formation, where the change of any cluster will not effect other clusters' utilities. Hence, the following condition is always satisfied with the transformation of the user structure:

$$U_{sum}(\mathcal{S}_a) < U_{sum}(\mathcal{S}_b), \tag{24}$$

where $U_{sum}(\mathcal{S}_a)$ is the sum utility of all users in structure $\mathcal{S}_a$. In other words, the sum utility of the user structure is strictly increased with the transformation in sequence (23). According to [39], the number of user structures is finite and equal to the Bell number, since there is a finite number of users. colorredTherefore, the user structure in sequence (23) can always converge to a local optimal structure. ■

3) Stability: In this paper, the stability of the proposed user clustering algorithms follows Nash-stable in [40] which can be defined as follows:

Definition 1: A user structure $\mathcal{S}$ is Nash-stable if for any DL or UL user i, where $i \in S_t, S_t \in \mathcal{S}$, the preference relation $S_t \succ_i S_{t'}$ is always satisfied for all $S_{t'} \in \mathcal{S} \cup \emptyset$.

According to the definition of Nash-stable, the stability of UCA-DL and UCA-UL can be present as follows:

Proposition 3: In the user clustering game $(\mathcal{J}, \mathcal{K}, U)$, any finial user structure achieved by UCA-DL and UCA-UL is Nash-stable.

Proof: The proposition can be proved by considering a situation that any final structure $\mathcal{S}_{final}$ is not Nash-stable. It means that there exist at least one user tends to swap to another cluster, which meets the condition of preference relation (22). More particularly, the sum utilities of these two changed clusters can be increased with the swap operation. Note that the utilities of all other clusters are not changed with this operation. Hence, the sum utility of all users in $\mathcal{S}_{final}$ is increased in this situation. It is contradicted to the fact that the final structure resulted by UCA-DL or UCA-UL cannot be improved. Therefore, any final structure comes from UCA-DL or UCA-UL is Nash-stable. ■

C. Problem Formulation: Power Allocation

Now that the UL and DL users are clustered based on the proposed clustering algorithms and we have the analytical expressions for SINR and PN-SINR, in this section we first formulate the PN-SINR maximization problem. Notice that unlike most prior work, we focus on a holistic optimization of UL and DL, where the total PN-SINR of the system is considered. This is particularly important due to the consideration of FD scenario. For HD scenario though, it is possible to do the optimization of only the UL or DL. However, for the sake of fairness, in this paper we consider fractions of DL and UL transmissions as η^{DL} and η^{UL}, respectively and holistically consider the PN-SINR for HD systems. The case with either $\eta^{DL} = 0$ or $\eta^{UL} = 0$ will signify the separate optimization case.

Using (17) and (19), the primal power allocation optimization problem for maximizing the PN-SINR for the FD NoMA can be formulated as

$$\begin{aligned}
(\mathbf{P1}) \max_{\mathcal{P}_D, \mathcal{P}_U} \; & \left[\frac{\Gamma^{DL} + \Gamma^{UL}}{\mathcal{P}_T} \right. \\
& \left. = \frac{\sum_{t=1}^{T} \left(\sum_{j=1}^{\widetilde{J}} \gamma_{t,j}^{DL} + \sum_{k=1}^{\widetilde{K}} \gamma_{t,k}^{UL} \right)}{\left\{ \sum_{t=1}^{T} \left(\sum_{j=1}^{\widetilde{J}} P_{D_{t,j}} + \sum_{k=1}^{\widetilde{K}} P_{U_{t,k}} \right) + P_{CP} \right\}} \right] \\
\text{s.t. } & (C.1) \sum\nolimits_{t=1}^{T} \sum\nolimits_{j=1}^{\widetilde{J}} P_{D_{t,j}} <= P_{DL}^{max}, \\
& (C.2) \sum\nolimits_{t=1}^{T} \sum\nolimits_{k=1}^{\widetilde{K}} P_{U_{t,k}} <= P_{UL}^{max}, \\
& (C.3) \; \gamma_{t,i \rightarrow j}^{DL} \geq \gamma_{D_{t,j}}^{min}, \qquad \forall j < i, j \neq \widetilde{J}, \forall S_t \in \mathcal{S}, \\
& (C.4) \; \gamma_{t,k}^{UL} \geq \gamma_{U_{t,k}}^{min}, \qquad \forall k \in \widetilde{K}, \forall S_t \in \mathcal{S},
\end{aligned} \tag{25}$$

where $\mathcal{P}_D = \{P_{D_{t,j}}, \; \forall t, j\}$, $\mathcal{P}_U = \{P_{U_{t,k}}, \; \forall t, k\}$ and $\gamma_{D_{t,j}}^{min}$ and $\gamma_{U_{t,k}}^{min}$ denote the minimum QoS of the jth DL and kth UL users in S_t cluster. Further, $\gamma_{t,j}^{DL}$, $\gamma_{t,k}^{UL}$, and $\gamma_{t,i \rightarrow j}^{DL}$ are defined in (8), and (11), and (19) respectively. Furthermore, $(C.1)$ constrains total DL power by a maximum BS transmit power budget $P_{DL}^{\max}$, and $(C.2)$ constrains the sum power of the UL users by maximum UL transmit power budget $P_{UL}^{\max}$, the constraint $(C.3)$ provides the fundamental condition for the implementation of SIC in DL NoMA, and the constraint $(C.4)$ are required to provide the minimum fairness for UL users.

The above problem is a non-convex nonlinear fractional programming problem [41]. Therefore, we first transform the original fractional problem into an equivalent non-fractional problem by exploiting the relationship between fractional and parametric programming problems [27], and then the equivalent non-fractional problem is solved through a dual-layer optimization scheme. While in the outer layer, the positive parameter ϕ, which works as penalty for resource utilization, is searched using a simple 1-D search, in the inner layer, the local optimal power allocation coefficients are found.

Proposition 4: Let $\mathcal{P} = \{\mathcal{P}_D, \mathcal{P}_U\}$ and $f_1(\mathcal{P}) = \sum_{t=1}^{T}\left(\sum_{j=1}^{\widetilde{J}}\gamma_{t,j}^{DL} + \sum_{k=1}^{\widetilde{K}}\gamma_{t,k}^{UL}\right)$ and $f_2(\mathcal{P}) = \mathcal{P}_T(\mathcal{P}) = \sum_{t=1}^{T}\left(\sum_{j=1}^{\widetilde{J}} P_{D_{t,j}} + \sum_{k=1}^{\widetilde{K}} P_{U_{t,k}}\right) + P_{CP}$. The optimal power allocation $\widetilde{\mathcal{P}}$ achieves the maximum penalty factor ϕ^* such that

$$\phi^* = \frac{f_1(\widetilde{\mathcal{P}})}{f_2(\widetilde{\mathcal{P}})} = \max_{\mathcal{P}} \frac{f_1(\mathcal{P})}{f_2(\mathcal{P})},$$

$$\iff \max_{\mathcal{P}} \{f_1(\mathcal{P}) - \phi^* f_2(\mathcal{P})\}$$
$$= f_1(\widetilde{\mathcal{P}}) - \phi^* f_2(\widetilde{\mathcal{P}}) = 0 \tag{26}$$

with $f_1(\mathcal{P}) > 0$ and $f_2(\mathcal{P}) > 0$.

It can be concluded from Proposition 4 that for any objective function in fractional form, there exists an equivalent objective function in subtractive form, which shares the same objective and constraint values. Accordingly, to find the optimal power allocation coefficients for given ϕ, the optimization problem (25) in fractional form can be solved by focusing on the following tractable subtractive form problem:

$$\begin{aligned}
(\mathbf{P2}) \max_{\mathcal{P}_D,\mathcal{P}_U} & \sum_{t=1}^{T}\left(\sum_{j=1}^{\widetilde{J}}\gamma_{t,j}^{DL} + \sum_{k=1}^{\widetilde{K}}\gamma_{t,k}^{UL}\right) \\
& - \phi\left\{\sum_{t=1}^{T}\left(\sum_{j=1}^{\widetilde{J}} P_{D_{t,j}} + \sum_{k=1}^{\widetilde{K}} P_{U_{t,k}}\right) + P_{CP}\right\} \\
\text{s.t.} \quad & (C.1)\ \sum_{t=1}^{T}\sum\nolimits_{j=1}^{\widetilde{J}} P_{D_{t,j}} <= P_{DL}^{max}, \\
& (C.2)\ \sum_{t=1}^{T}\sum\nolimits_{k=1}^{\widetilde{K}} P_{U_{t,k}} <= P_{UL}^{max}, \\
& (C.3)\ \gamma_{t,i\to j}^{DL} \geq \gamma_{D_{t,j}}^{min},\ \forall j < i, j \neq \widetilde{J}, \forall S_t \in \mathcal{S}\,, \\
& (C.4)\ \gamma_{t,k}^{UL} \geq \gamma_{U_{t,i}}^{min}, \quad \forall k \in \widetilde{K}, \forall S_t \in \mathcal{S}\,.
\end{aligned} \tag{27}$$

The problem (**P2**) in (27) is still non-convex due to the presence of the optimization variables in the denominator of $\gamma_{t,j}^{DL}$ and $\gamma_{t,k}^{UL}$. However, the non-convex problem (**P2**) can be converted into a convex form by introducing auxiliary variables $\Omega_{t,j}^{DL} = |h_{t,j}^{DL}|^2 \sum_{i=j+1}^{\widetilde{J}} P_{D_{t,i}} + \kappa \sum_{i=1,i\neq j}^{\widetilde{J}} P_{D_{t,i}} |h_{t,j}^{DL}|^2 + (1+\kappa)\sum_{k=1}^{\widetilde{K}} P_{U_{t,k}} |h_{t,jk}^{DU}|^2 + \beta\Psi_j^{DL}$ and $\Omega_{t,k}^{UL} = \sum_{i=1,i>k}^{\widetilde{K}} P_{U_{t,i}} |h_{t,i}^{UL}|^2 + \kappa \sum_{i=1}^{\widetilde{K}} P_{U_{t,i}} |h_{t,i}^{UL}|^2 + \kappa \sum_{j=1}^{\widetilde{J}} P_{D_{t,j}} |h_0|^2 + \beta \sum_{i=1}^{\widetilde{K}} P_{U_{t,i}} |h_{t,i}^{UL}|^2$, yielding (28), as shown on the top of the next page, where $\mathbf{\Omega}^{DL} = \{\Omega_{t,j}^{DL}, \forall t, j\}$ and $\mathbf{\Omega}^{UL} = \{\Omega_{t,k}^{UL}, \forall t, k\}$. Note that for fixed $\Omega_{t,j}^{DL}$, $\Omega_{t,k}^{UL}$, and penalty factor ϕ, the optimization problem (**P2**) is concave in variables $P_{D_{t,j}}$ and $P_{U_{t,k}}$ and thus, it can be solved using the standard convex optimization techniques [41]. The details on how to update the penalty factor ϕ and the auxiliary variables are described below.

1) Update of ϕ: In the objective function of (28), we can point out that there is a trade-off between the PN-SINR and SINR by adjusting the penalty factor ϕ. In result, we need to find the optimal penalty factor $\phi^\star$ in order to achieve the maximum PN-SINR of the considered network. Thus, the penalty factor in the $(l+1)$th iteration can be updated as

$$\phi(l+1) = \frac{\sum_{t=1}^{T}\sum_{j=1}^{\widetilde{J}} \frac{P_{D_{t,j}}^{\star}(l)|h_{t,j}^{DL}|^2}{\Omega_{t,j}^{DL\star}(l)+\sigma^2} + \sum_{t=1}^{T}\sum_{k=1}^{\widetilde{K}} \frac{P_{U_{t,k}}^{\star}(l)|h_{t,k}^{UL}|^2}{\Omega_{t,k}^{UL\star}(l)+\sigma^2}}{\mathcal{P}_T(\mathcal{P}_D^{\star}(l), \mathcal{P}_U^{\star}(l))}\,. \tag{29}$$

Algorithm 3 An iterative power allocation algorithm

1: **Input:** Convergence tolerance ϵ_{out}.
2: Initialize the iteration counter $l = 0$ and penalty factor $\phi[0] \leftarrow 0$.
3: **do while** $\phi(l) - \phi(l-1) \geq \epsilon_{out}$
4: Solve the problem (**P2**) to get $\left(\mathcal{P}_D^{\star}, \mathcal{P}_U^{\star}, \mathbf{\Omega}^{DL^\star}, \mathbf{\Omega}^{UL^\star}\right)$.
5: Update $\phi(l+1)$ using (29).
6: Set $\mathcal{P}_D(l+1) \leftarrow \mathcal{P}_D^{\star}$, $\mathcal{P}_U(l+1) \leftarrow \mathcal{P}_U^{\star}$, and set $l \leftarrow l+1$.
7: **end do**
8: **return** $\left(\phi^\star, \mathcal{P}_D^{\star}, \mathcal{P}_U^{\star}, \mathbf{\Omega}^{DL^\star}, \mathbf{\Omega}^{UL^\star}\right)$.

Lemma 1: Let $\left(\mathcal{P}_D^{\star}, \mathcal{P}_U^{\star}\right)$ be the optimal power allocation policy for the problem (**P1**) with respect to $\phi^\star$. If this optimal power allocation policy satisfies the following balance equation:

$$\sum_{t=1}^{T}\sum_{j=1}^{\widetilde{J}} \frac{P_{D_{t,j}}^{\star}|h_{t,j}^{DL}|^2}{\Omega_{t,j}^{DL\star}+\sigma^2} + \sum_{t=1}^{T}\sum_{k=1}^{\widetilde{K}} \frac{P_{U_{t,k}}^{\star}|h_{t,k}^{UL}|^2}{\Omega_{t,k}^{UL\star}+\sigma^2} - \phi^\star \mathcal{P}_T(\mathcal{P}_D^{\star}, \mathcal{P}_U^{\star}) = 0\,, \tag{30}$$

then $\phi^\star$ will be the optimal.

Proposition 5: Suppose $\left(\mathcal{P}_D^{\star}(l), \mathcal{P}_U^{\star}(l)\right)$ is the local maximizer of the problem (**P1**) for given $\phi(l)$ in the lth iteration and if the penalty factor is updated at the $(l+1)$th iteration using (29), then $\phi(l)$ is monotonically increasing with respect to l and when it converges, the penalty at the converged point is the optimal price, i.e., $\phi^\star = \lim_{l\to\infty}\phi(l)$ satisfies the balance equation.

Proof: Let $\mathcal{F}(\phi(l)) = \sum_{t=1}^{T}\sum_{j=1}^{\widetilde{J}} \frac{P_{D_{t,j}}^{\star}(l)|h_{t,j}^{DL}|^2}{\Omega_{t,j}^{DL\star}(l)+\sigma^2} + \sum_{t=1}^{T}\sum_{k=1}^{\widetilde{K}} \frac{P_{U_{t,k}}^{\star}(l)|h_{t,k}^{UL}|^2}{\Omega_{t,k}^{UL\star}(l)+\sigma^2} - \phi(l)\mathcal{P}_T(\mathcal{P}_D^{\star}(l), \mathcal{P}_U^{\star}(l))$. From the definition of $\phi(l+1)$ in (29), we have

$$\begin{aligned}
&\phi(l+1)\mathcal{P}_T(\mathcal{P}_D^{\star}(l), \mathcal{P}_U^{\star}(l)) \\
&= \sum_{t=1}^{T}\sum_{j=1}^{\widetilde{J}} \frac{P_{D_{t,j}}^{\star}(l)|h_{t,j}^{DL}|^2}{\Omega_{t,j}^{DL\star}(l)+\sigma^2} + \sum_{t=1}^{T}\sum_{k=1}^{\widetilde{K}} \frac{P_{U_{t,k}}^{\star}(l)|h_{t,k}^{UL}|^2}{\Omega_{t,k}^{UL\star}(l)+\sigma^2}\,.
\end{aligned} \tag{31}$$

Using (31), $\mathcal{F}(\phi(l))$ can be written as

$$\begin{aligned}
\mathcal{F}(\phi(l)) &= \sum_{t=1}^{T}\sum_{j=1}^{\widetilde{J}} \frac{P_{D_{t,j}}^{\star}(l)|h_{t,j}^{DL}|^2}{\Omega_{t,j}^{DL\star}(l)+\sigma^2} + \sum_{t=1}^{T}\sum_{k=1}^{\widetilde{K}} \frac{P_{U_{t,k}}^{\star}(l)|h_{t,k}^{UL}|^2}{\Omega_{t,k}^{UL\star}(l)+\sigma^2} \\
&\quad - \phi(l)\left(\mathcal{P}_T(\mathcal{P}_D^{\star}(l), \mathcal{P}_U^{\star}(l))\right) \\
&= \phi(l+1)\mathcal{P}_T(\mathcal{P}_D^{\star}(l), \mathcal{P}_U^{\star}(l)) - \phi(l)\left(\mathcal{P}_T(\mathcal{P}_D^{\star}(l), \mathcal{P}_U^{\star}(l))\right) \\
&= \mathcal{P}_T(\mathcal{P}_D^{\star}(l), \mathcal{P}_U^{\star}(l)) \cdot (\phi(l+1) - \phi(l)) \geq 0\,.
\end{aligned} \tag{32}$$

$$
\begin{aligned}
(\mathbf{P3}) \quad & \max_{\substack{\mathcal{P}_D,\mathcal{P}_U \\ \mathbf{\Omega}^{DL},\mathbf{\Omega}^{UL}}} \sum\nolimits_{t=1}^{T}\sum\nolimits_{j=1}^{\widetilde{J}} \frac{P_{D_{t,j}}|h_{t,j}^{DL}|^2}{\Omega_{t,j}^{DL}+\sigma^2} + \sum\nolimits_{t=1}^{T}\sum\nolimits_{k=1}^{\widetilde{K}} \frac{P_{U_{t,k}}|h_{t,k}^{UL}|^2}{\Omega_{t,k}^{UL}+\sigma^2} - \phi * \mathcal{P}_T(\mathcal{P}_D,\mathcal{P}_U) \\
& \text{s.t.} \quad (C.1)-(C.2)\ , \\
& \quad (C.3)\ P_{D_{t,j}}|h_{t,i}^{DL}|^2 \geq \gamma_{D_{t,j}}^{min}\Bigg(|h_{t,i}^{DL}|^2\sum\nolimits_{l=j+1}^{\widetilde{J}} P_{D_{t,l}} + \kappa\sum\nolimits_{l=1,l\neq i}^{\widetilde{J}} P_{D_{t,l}}|h_{t,i}^{DL}|^2 \\
& \qquad\qquad +(1+\kappa)\sum\nolimits_{k=1}^{\widetilde{K}} P_{U_{t,k}}|h_{t,jk}^{DU}|^2 + \beta\Psi_i^{DL} + \sigma^2\Bigg)\ , \quad \forall j<i, j\neq\widetilde{J}, \forall S_t\in\mathcal{S}\,, \\
& \quad (C.4)\ P_{U_{t,k}}|h_{t,k}^{UL}|^2 \geq \gamma_{U_{t,k}}^{min}\left(\Omega_{t,k}^{UL}+\sigma^2\right)\ , \qquad \forall k\in\widetilde{K}, \forall S_t\in\mathcal{S}\,, \\
& \quad (C.5)\ |h_{t,j}^{DL}|^2\sum\nolimits_{i=j+1}^{\widetilde{J}} P_{D_{t,i}} + \kappa\sum\nolimits_{i=1,i\neq j}^{\widetilde{J}} P_{D_{t,i}}|h_{t,j}^{DL}|^2 \\
& \qquad\qquad + (1+\kappa)\sum\nolimits_{k=1}^{\widetilde{K}} P_{U_{t,k}}|h_{t,jk}^{DU}|^2 + \beta\Psi_j^{DL} \leq \Omega_{t,j}^{DL}\ , \quad \forall j\in\widetilde{J}, \forall S_t\in\mathcal{S}\,, \\
& \quad (C.6)\ \sum\nolimits_{i=1,i>k}^{\widetilde{K}} P_{U_{t,i}}|h_{t,i}^{UL}|^2 + \kappa\sum\nolimits_{i=1}^{\widetilde{K}} P_{U_{t,i}}|h_{t,i}^{UL}|^2 \\
& \qquad\qquad + \kappa\sum\nolimits_{j=1}^{\widetilde{J}} P_{D_{t,j}}|h_0|^2 + \beta\sum\nolimits_{i=1}^{\widetilde{K}} P_{U_{t,i}}|h_{t,i}^{UL}|^2 \leq \Omega_{t,k}^{UL}\ , \quad \forall k\in\widetilde{K}, \forall S_t\in\mathcal{S}\,.
\end{aligned} \tag{28}
$$

Note that the power consumption $\mathcal{P}_T(\mathcal{P}_D^\star(l),\mathcal{P}_U^\star(l)) \geq 0$, it implies that $\phi\,(l+1) \geq \phi\,(l)$. Since the penalty factor ϕ is monotonically increasing with respect to l.

To prove the second part, we use contradiction method. Let the penalty factor converges at $\breve{\phi}$, i.e., $\phi(l) = \phi(l+1) = \breve{\phi}$, however $\breve{\phi}$ is not the optimal. Then, the balance equation in Lemma 1 will not be hold:

$$
\begin{aligned}
\sum_{t=1}^{T}\sum_{j=1}^{\widetilde{J}} \frac{P_{D_{t,j}}^\star(l)|h_{t,j}^{DL}|^2}{\Omega_{t,j}^{DL^\star}(l)+\sigma^2} + \sum_{t=1}^{T}\sum_{k=1}^{\widetilde{K}} \frac{P_{U_{t,k}}^\star(l)|h_{t,k}^{UL}|^2}{\Omega_{t,k}^{UL^\star}(l)+\sigma^2} \\
- \phi(l)\left(\mathcal{P}_T(\mathcal{P}_D^\star(l),\mathcal{P}_U^\star(l))\right) \neq 0\,.
\end{aligned} \tag{33}
$$

Consequently, from (29) and (33), we have (34), as shown on the top of the next page, which contradicts the declaration of $\phi(l) = \phi(l+1)$. ∎

2) Update of $\mathbf{\Omega}^{DL}$ and $\mathbf{\Omega}^{UL}$: We need to determine the values of the auxiliary variables $\mathbf{\Omega}^{DL}$ and $\mathbf{\Omega}^{UL}$ in order to maximize the PN-SINR, expressed by (35), as shown on the next page. An exhaustive search (ES) method can apply to find the optimal $\mathbf{\Omega}^{DL^\star}$ and $\mathbf{\Omega}^{UL^\star}$ by searching variables over all values of $\Omega_{t,j}^{DL}$, $\forall j \in \widetilde{J}, \forall S_t \in \mathcal{S}$ and $\Omega_{t,k}^{UL}$, $\forall k \in \widetilde{K}, \forall S_t \in \mathcal{S}$. However, the computational complexity will be very high for higher number of UL and DL users. Instead, we propose a two-step method to find the values of $\Omega_{t,j}^{DL}$, $\forall j \in \widetilde{J}, \forall S_t \in \mathcal{S}$ and $\Omega_{t,k}^{UL}$, $\forall k \in \widetilde{K}, \forall S_t \in \mathcal{S}$. We firstly initialize the auxiliary variables $\Omega_{t,j}^{DL}$ and $\Omega_{t,k}^{UL}$, for $\forall j \in \widetilde{J}, \forall k \in \widetilde{K}, \forall S_t \in \mathcal{S}$ by generating a random number between 0 and 1, and find the corresponding optimal power allocation policy $(\mathcal{P}_D^\star, \mathcal{P}_U^\star))$. In a next step, we update the auxiliary variables as $\Omega_{t,j}^{DL} = |h_{t,j}^{DL}|^2\sum_{i=j+1}^{\widetilde{J}} P_{D_{t,i}}^\star + \kappa\sum_{i=1,i\neq j}^{\widetilde{J}} P_{D_{t,i}}^\star|h_{t,j}^{DL}|^2 + (1+\kappa)\sum_{k=1}^{\widetilde{K}} P_{U_{t,k}}^\star|h_{t,jk}^{DU}|^2 + \beta\Psi_j^{DL^\star}$ and $\Omega_{t,k}^{UL} = \sum_{i=1,i>k}^{\widetilde{K}} P_{U_{t,i}}^\star|h_{t,i}^{UL}|^2 + \kappa\sum_{i=1}^{\widetilde{K}} P_{U_{t,i}}^\star|h_{t,i}^{UL}|^2 + \kappa\sum_{j=1}^{\widetilde{J}} P_{D_{t,j}}^\star|h_0|^2 + \beta\sum_{i=1}^{\widetilde{K}} P_{U_{t,i}}^\star|h_{t,i}^{UL}|^2$, for $\forall j \in \widetilde{J}, \forall k \in \widetilde{K}, \forall S_t \in \mathcal{S}$.

The proposed iterative power allocation is described as follows. Note that the optimization problem (**P3**) can be solved in two steps. We first initialize the penalty factor $\phi = 0$ and set $\Omega_{t,j}^{DL} = 0$, and $\Omega_{t,k}^{UL} = 0$ and compute the corresponding power solution $\mathcal{P}_D$ and $\mathcal{P}_U$. Next, we solve the problem (**P3**) for given penalty factor ϕ to get a near-optimal/local optimal solution $(\mathcal{P}_D^\star, \mathcal{P}_U^\star)$. In the next step, based on the obtained solution, we then refine the optimal power solution by updating the auxiliary variables as $\Omega_{t,j}^{DL} = |h_{t,j}^{DL}|^2\sum_{i=j+1}^{\widetilde{J}} P_{D_{t,i}}^\star + \kappa\sum_{i=1,i\neq j}^{\widetilde{J}} P_{D_{t,i}}^\star|h_{t,j}^{DL}|^2 + (1+\kappa)\sum_{k=1}^{\widetilde{K}} P_{U_{t,k}}^\star|h_{t,jk}^{DU}|^2 + \beta\Psi_j^{DL^\star}$ and $\Omega_{t,k}^{UL} = \sum_{i=1,i>k}^{\widetilde{K}} P_{U_{t,i}}^\star|h_{t,i}^{UL}|^2 + \kappa\sum_{i=1}^{\widetilde{K}} P_{U_{t,i}}^\star|h_{t,i}^{UL}|^2 + \kappa\sum_{j=1}^{\widetilde{J}} P_{D_{t,j}}^\star|h_0|^2 + \beta\sum_{i=1}^{\widetilde{K}} P_{U_{t,i}}^\star|h_{t,i}^{UL}|^2$. This enables us to refine the solutions of the power allocation by following the track of the optimal accumulated power expenditure profiles $\Omega_{t,j}^{DL}$, and $\Omega_{t,k}^{UL}$. With the refined power allocation solution $\mathcal{P}_D$ and $\mathcal{P}_U$, we update the penalty factor ϕ using (29). We repeat this procedure until the convergence of the power allocation algorithm or the iteration counter reaches the maximum limit. Due to the local optimality of the proposed ϕ-penalty based algorithm, the optimal penalty $\phi^\star$ found in this algorithm can only guarantee that the locally optimum power allocation in (**P1**) with respect to $\phi^\star$ is a local maximizer of the PN-SINR. The iterative algorithm is summarized in Algorithm 3.

V. Numerical Results

In this section, we evaluate the performance of the proposed PN-SINR maximization algorithm through extensive computer simulations. The 3GPP-based path loss model given by $131.1+42.8\times\log_{10}(d)$ dB, (d: distance in kilometers) [42] is adopted. Here the maximum number of iterations of the iterative algorithm is set at 15 and the convergence tolerance value is set as 10^{-5}, while the bandwidth is kept at 10 MHz. The deployment FD technology is more suitable for small cell because of its low transmit power, low mobility and short transmission distances. The maximum number of resource blocks is greater than or equal to the number of users, i.e., $T_{max} \geq J+K$. That is, all users can be allocated into different resource blocks in an extreme case. The unoccupied resource

$$\phi\left(l\right) \neq \frac{\sum_{t=1}^{T}\sum_{j=1}^{\widetilde{J}} \frac{P^{\star}_{D_{t,j}}(l)|h^{DL}_{t,j}|^2}{\Omega^{DL^{\star}}_{t,j}(l)+\sigma^2} + \sum_{t=1}^{T}\sum_{k=1}^{\widetilde{K}} \frac{P^{\star}_{U_{t,k}}(l)|h^{UL}_{t,k}|^2}{\Omega^{UL^{\star}}_{t,k}(l)+\sigma^2}}{\mathcal{P}_T(\mathcal{P}^{\star}_D(l), \mathcal{P}^{\star}_U(l))} = \phi\left(l+1\right), \tag{34}$$

$$\left[\boldsymbol{\Omega}^{DL^{\star}}, \boldsymbol{\Omega}^{UL^{\star}}\right] = \arg \max_{\boldsymbol{\Omega}^{DL}, \boldsymbol{\Omega}^{UL}} \sum_{t=1}^{T}\sum_{j=1}^{\widetilde{J}} \frac{P^{\star}_{D_{t,j}}|h^{DL}_{t,j}|^2}{\Omega^{DL}_{t,j}+\sigma^2} + \sum_{t=1}^{T}\sum_{k=1}^{\widetilde{K}} \frac{P^{\star}_{U_{t,k}}|h^{UL}_{t,k}|^2}{\Omega^{UL}_{t,k}+\sigma^2} - \phi^{\star}\mathcal{P}_T(\mathcal{P}^{\star}_D, \mathcal{P}^{\star}_U). \tag{35}$$

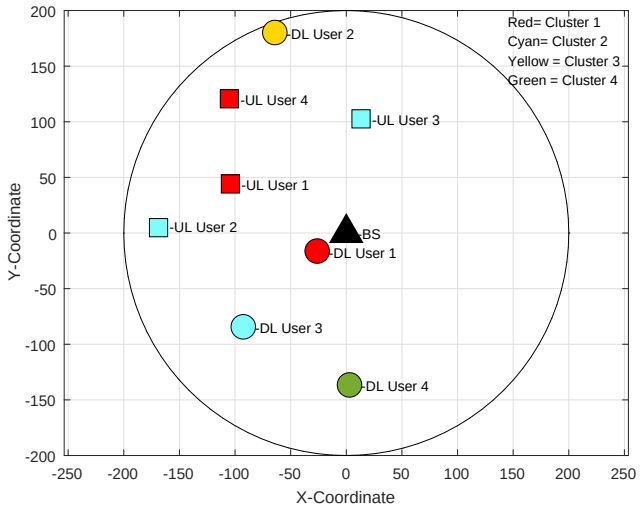

(a) $J = K = 4$

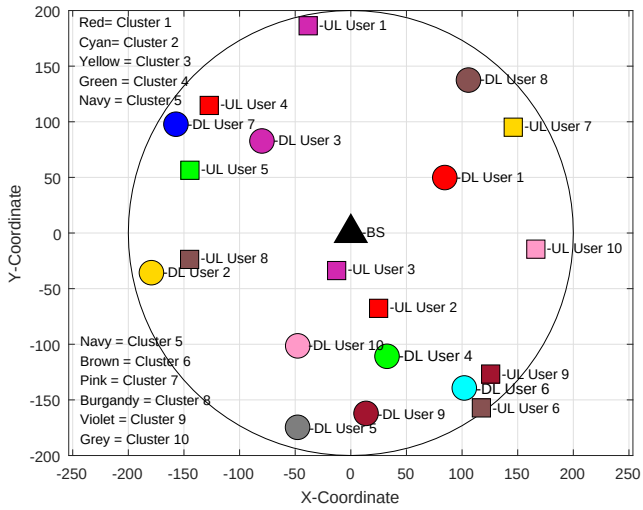

(b) $J = K = 10$

Fig. 2: Clustering of UL and DL users in a cell.

blocks are ignored since there is no bandwidth resource allocated to them. If T resource blocks are occupied by the users, where $T \leq T_{max}$, the bandwidth resource (time/frequency) of each cluster is $1/T$.

In the simulation, a single hexagonal cell is considered with cell radius $R = 200$m as illustrated in Fig. 2 for $P^{max}_{DL} = 20$dBm, $J = K = 4$ and $J = K = 10$ users, where the BS is located at origin. Each user in the cell is equpped with a single antenna. Using Algorithm 1 and Algorithm 2, all the DL and UL users are allocated into clusters, as indicated in Fig. 2 by various shapes and colours. In particular, the user structure in Fig. 2.(a) can be expressed as $\mathcal{S} = \{\{1^{DL}, 1^{UL}, 4^{UL}\}, \{2^{DL}\}, \{3^{DL}, 1^{UL}, 4^{UL}\}, \{4^{DL}\}\}$, where $j^{DL}, \forall j \in \mathcal{J}$ and $k^{UL}, \forall k \in \mathcal{K}$ denote the DL and UL users, respectively. The BS is equipped with two antennas, one antenna for transmission and other for reception, and it operates in FD mode [2]. Further, we consider the thermal noise density of -174 dBm/Hz while the value of shadow fading standard deviation is set at 8dB. The Rician model in [43] is adopted for modelling the SI channel. The values of transmitter(receiver) distortion parameters $\kappa(\beta)$, which refer to RSI cancellation is set as $\kappa = \beta = -90$dB. Unless otherwise stated, we set the values of $J = K = 4$, $R = 200$m, $P^{max}_{UL} = 5$dB, $P^{C}_{BS} = P^{C}_{U} = P_{Fix} = P_{LO_{BS}} = P_{LO_{U}} = 7.5$dB and the minimum QoS for DL and UL users as $\gamma^{min}_{D_{t,j}} = 10$dB and $\gamma^{min}_{U_{t,k}} = 5$dB, respectively. As a benchmark for comparison, we simulate HD-NoMA and the conventional OMA algorithm for the considered framework. In particular, in HD-NoMA, there is no SI and CCI due to the UL and DL operation happening in two different time slots. Hence, Algorithm 1 and 2 will put all the UL and DL users in a single cluster. The eventual calculation of SINR for the HD case follows [44]. In particular, the total sum-rate R is first divided by 2 because of the two time-slots transmission, from which the SINR is re-calculated as $2^{\frac{R}{2}} - 1$. Similarly, for the case of FD OMA, we follow traditional OMA systems, e.g., frequency division multiple access (FDMA) or time division multiple access (TDMA), where time/frequency resource allocation is non-adaptively divided into a fixed number of sub-channels to be orthogonally and equally shared by the users. In other words, each user is allocated with a fixed sub-channel by assuming equal resource (time or frequency) allocation to all users. The calculation of FD OMA follows from [44] after the CCI is attenuated through Algorithm 1 and 2, i.e., for any cluster S_t, with $\tilde{J}$ DL users and $\tilde{K}$ UL users, the SINR for OMA is calculated by first ignoring the interference terms and then dividing the sum-rate by $\frac{1}{\tilde{J}+\tilde{K}}$ because of equal allocation of the channel resources between the UL and DL users in the cluster, from which the SINR is re-calculated as $2^{\frac{R}{\tilde{J}+\tilde{K}}} - 1$.

We start with evolution of the proposed users' clustyering Algorithm 1 and Algorithm 2, and iterative power allocation algorithm given in Algorithm 3. The convergence behavior of the proposed clustering Algorithm 1 for DL users and Algorithm 2 for UL users is demonstrated in Fig. 3 for

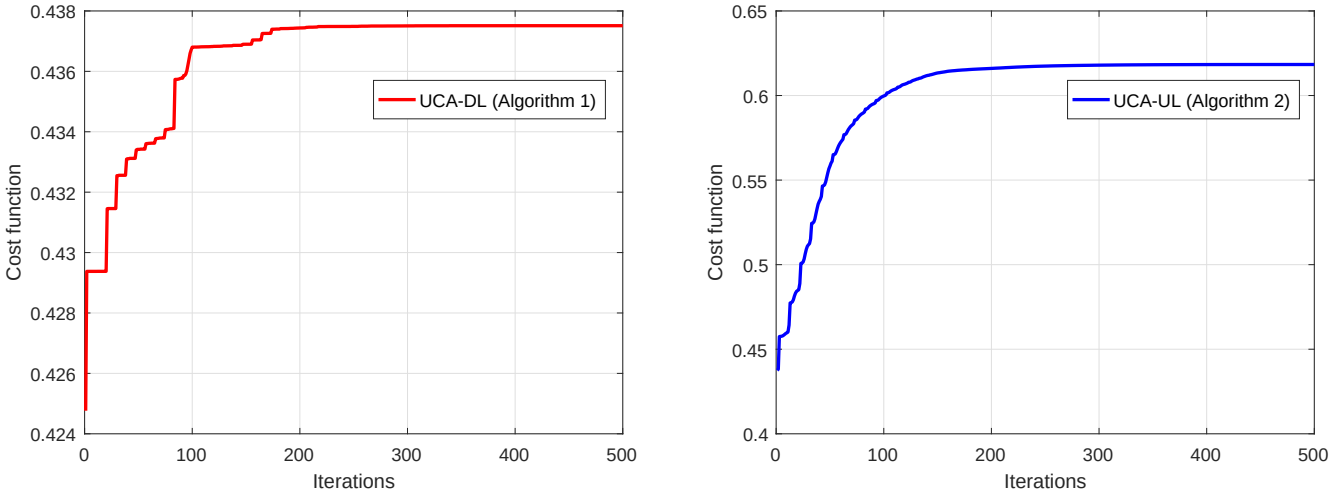

(a) (b)

Fig. 3: Convergence behaviour of the clustering Algorithm 1 (Left) and Algorithm 2 (Right).

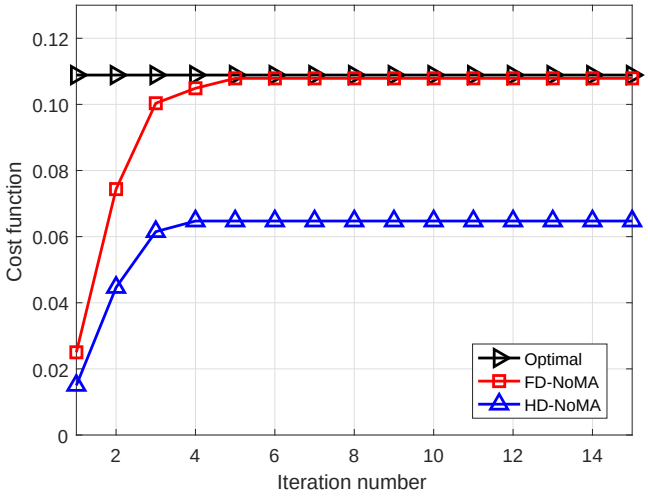

Fig. 4: Convergence behavior of the proposed power allocation algorithm.

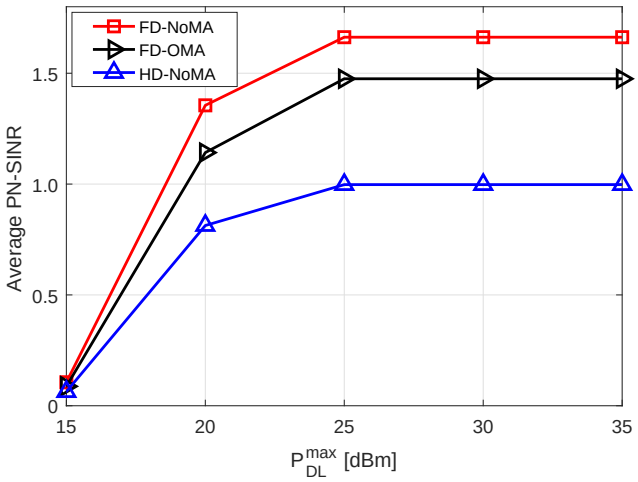

Fig. 5: Average PN-SINR versus P_{DL}^{max}.

$P_{DL}^{max} = 20$dBm, $J = K = 4$. It can be observed that the cost functions increases monotonically and converges within 250 iterations for both Algorithm 1 and Algorithm 2. Further, to demonstrate the convergence of the proposed power allocation algorithm, the parameter setting are as follows: $P_{DL}^{max} = 15$dB, $\kappa = \beta = -90$dB, $\gamma_{D_{t,j}}^{min} = 10$dB and $\gamma_{U_{t,k}}^{min} = 5$dB, respectively. We compare the performance of FD-NoMA with the optimum solution obtained by the exhaustive search (ES) method. Fig. 4 shows that the cost function PN-SINR increases monotonically and converges to the optimal solution within six iterations.

Fig. 5 illustrates the average PN-SINR of the proposed algorithm for different P_{DL}^{max} with $\kappa = \beta = -90$dB. We can observe that the average performance of FD-NoMA, FD-OMA and HD-NoMA increases as P_{DL}^{max} increases. In a low power regime i.e., $P_{DL}^{max} < 25$dBm, the performance is significantly improved with increasing P_{DL}^{max}, while it becomes steady in a high power regime i.e., $P_{DL}^{max} \geq 25$dBm. It can be noticed that the performance gap between FD-NoMA and FD-OMA becomes more in the higher power regime because of the better resource utilization. In addition, the FD-NoMA outperforms the HD-NoMA.

Fig. 6 shows the impact of transmitter/receiver distortion on average PN-SINR performance of the proposed algorithm. It can be observed that when the level of transmitter/receiver distortion increases from $\kappa = \beta = -90$dB to $\kappa = \beta = -60$dB, the performance of the proposed algorithm decreases rapidly in high power regime due to the fact that the RSI cancellation capability of the system becomes less at $\kappa = \beta = -60$dB. However, the proposed algorithm under FD-NoMA always outperforms the FD-OMA.

Fig. 7 shows the average PN-SINR performance of proposed algorithm under NoMA and OMA scenarios versus number of UL and DL users with $P_{DL}^{max} = 15$dB and $\kappa = \beta = -90$dB. For sake of simplicity, we consider $J = K$. In this figure, we can see that the average PN-SINR performance of the algorithm increases rapidly as $J = K$ increases specially

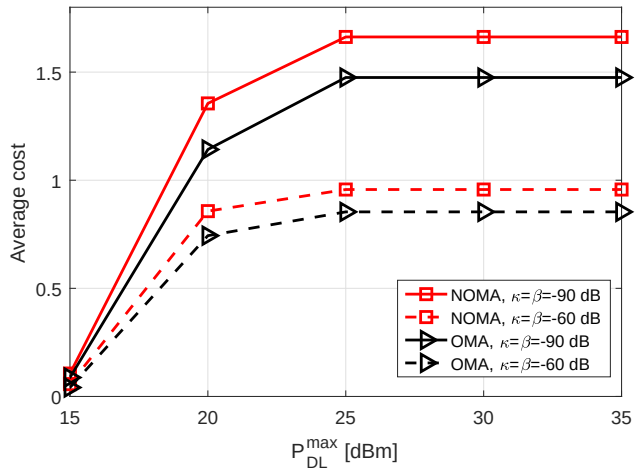

Fig. 6: Impact of transmitter/receiver distortion ($\kappa = \beta$) [dB] on average PN-SINR.

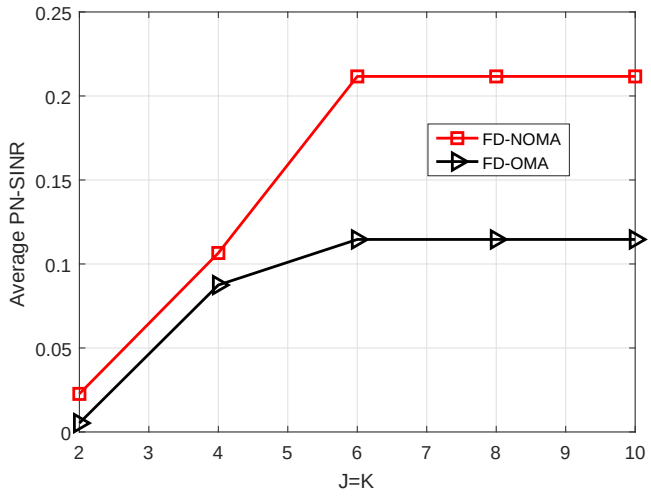

Fig. 7: Impact of number of users ($J = K$) on average PN-SINR.

for $J = K \leq 6$ and it becomes steady after $J = K \geq 6$. For $J = K \leq 6$, we achieve significant improvement in average PN-SINR due to multiuser diversity gain. However, for $J = K > 6$, since the transmit power for UL and DL users are fixed, increasing the number of UL and DL users does not help in improving the performance because the allocated transmit power to users becomes very limited.

Fig. 8 shows the EE performance of the proposed algorithm under FD-NoMA and FD-OMA for different transmitter/receiver distortion. In this figure, we can see that the EE of the proposed algorithm under FD-NoMA is decreasing as P_{DL}^{max} increases. However, the EE performance of the FD-NoMA is much better than FD-OMA scheme. Note that the higher EE can be achieved in low power regime for both FD-NoMA and FD-OMA due to less RSI.

VI. Conclusion

We formulated a user clustering optimization problem to mitigate the CCI under the constraint of SIC and the binary constraints for the allocations of UL and DL users, respectively. By adopting a game theoretic approach, we proposed the clustering algorithms for UL and DL users and provided

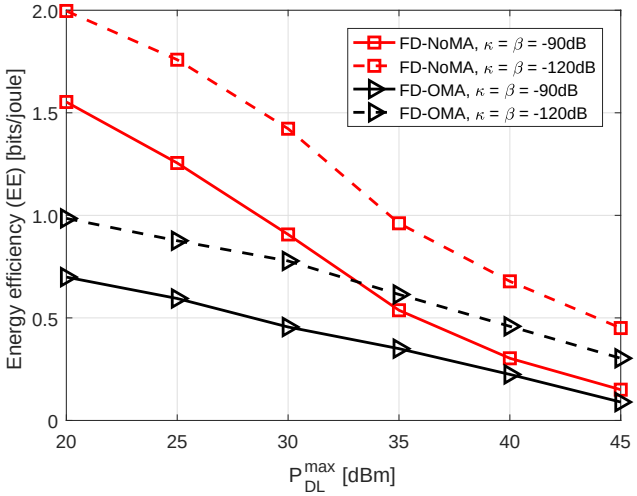

Fig. 8: Energy Efficiency versus P_{DL}^{max}

the analysis of complexity, convergence, and the stability of the clustering algorithms. Further, we formulated the PN-SINR maximization problem for controlling the RSI under the constraints of the total transmit power budget at the BS and UL users, the fundamental condition for the implementation of SIC in DL NoMA, and the minimum fairness condition for UL users. The original PN-SINR maximization fractional problem was then converted into an equivalent subtractive-form problem by exploiting the properties of fractional programming and dual-layer optimization scheme. Finally, we proposed an iterative algorithm to obtain the optimal power allocation policy which maximizes the PN-SINR of the FD-NoMA system. Simulation results demonstrated the superiority of FD-NoMA over HD-NoMA and the conventional FD-OMA in terms of average PN-SINR and EE.

At this point, it is worth noting that the system model in this paper considers a single cell scenario. The extension to multi-cells systems will be considered in the near future. Further, imperfect CSI and its impacts on user clustering and power allocation for the proposed framework will also be considered in future works.

References

[1] H. Ju, E. Oh and D. Hong, "Catching resource-devouring worms in next-generation wireless relay systems: Two-way relay and full-duplex relay," *IEEE Commun. Mag.*, vol. 47, no. 9, pp. 58-65, Sept. 2009.

[2] D. Bharadia, E. McMilin, and S. Katti, "Full duplex radios," in *Proc. ACM Conf. SIGCOMM*, Hong Kong, Aug. 2013, pp. 375-386.

[3] B. P. Day, A. R. Margetts, D. W. Bliss, and P. Schniter, "Full-duplex bidirectional MIMO: Achievable rates under limited dynamic range," *IEEE Trans. Signal Process.*, vol. 60, no. 7, pp. 3702-3713, Jul. 2012.

[4] M. Jain, J. I. Choi, T. Kim, D. Bharadia, K. Srinivasan, S. Seth, P. Levis, S. Katti, and P. Sinha, "Practical, real-time, full duplex wireless," in *Proc. Mobicom*, USA, Sept. 2011, pp. 301-312.

[5] M. Al-Imari, P. Xiao, M. A. Imran, and R. Tafazolli, "Uplink non-orthogonal multiple access for 5G wireless networks," *in Proc. IEEE Int. Symp. Wireless Commun. Syst. (ISWCS)*, Barcelona, Spain, Aug. 2014, pp. 781-785.

[6] N. Zhang, J.Wang, G. Kang, and Y. Liu, "Uplink nonorthogonal multiple access in 5G systems," *IEEE Commun. Lett.*, vol. 20, no. 3, pp. 458-461, Mar. 2016.

[7] Z. Ding, P. Fan, and V. Poor, "Impact of user pairing on 5G non-orthogonal multiple access downlink transmissions," *IEEE Trans. Veh. Technol.*, vol. 65, no. 8, pp. 6010-6023, Aug. 2016.

[8] Z. Ding, Z. Yang, P. Fan, and H. V. Poor, "On the performance of non-orthogonal multiple access in 5G systems with randomly deployed users," *IEEE Signal Process. Lett.*, vol. 21, no. 12, pp. 1501-1505, Dec.2014.

[9] M. F. Hanif, Z. Ding, T. Ratnarajah, and G. K. Karagiannidis, "A minorization-maximization method for optimizing sum rate in the downlink of non-orthogonal multiple access systems," *IEEE Trans. Veh. Technol.*, vol. 64, no. 1, pp. 76-88, Jan. 2016.

[10] Z. Ding and R. Schober and H. V. Poor, "A General MIMO Framework for NOMA Downlink and Uplink Transmission Based on Signal Alignment," *IEEE Trans. Wireless Commun.*, vol. 15, no. 6, pp. 4438-4454, Jun. 2016.

[11] A. C. Cirik, S. Biswas, S. Vuppala, and T. Ratnarajah, "Beamforming design for full-duplex MIMO interference channels QoS and energy-efficiency considerations," *IEEE Trans. Commun.*, vol. 64, no. 11, pp. 4635-4651, Nov. 2016.

[12] A. C. Cirik, S. Biswas, O. Taghizadeh, and T. Ratnarajah, "Robust transceiver design in full-duplex MIMO cognitive radios," *IEEE Trans. Veh. Technol.*, vol: 67, no 2, pp. 1313-1330, Feb. 2018.

[13] A. C. Cirik, S. Biswas, S. Vuppala, and T. Ratnarajah, "Robust transceiver design for full duplex multiuser MIMO systems," *IEEE Wireless Commun. Let.*, vol. 5, no. 3, pp. 260-263, Jun. 2016.

[14] S. Biswas, K. Singh, O. Taghizadeh, and T. Ratnarajah, "Coexistence of MIMO radar and FD MIMO cellular systems with QoS considerations," *IEEE Trans. Wireless Commun.*, vol. 17, no. 11, pp. 7281-7294, Nov. 2018.

[15] Y. Liu, Z. Qin, M. Elkashlan, Z. Ding, A. Nallanathan, and L. Hanzo, "Nonorthogonal multiple access for 5G and beyond," *Proc. IEEE*, vol. 105, no. 12, pp. 2347-2381, Dec. 2017.

[16] Z. Qin, X. Yue, Y. Liu, Z. Ding, and A. Nallanathan, "User association and resource allocation in unified NOMA enabled heterogeneous ultra dense networks," *IEEE Commun. Magazine*, vol. 56, no. 6, pp. 86-92, Jun. 2018.

[17] Z. Ding, Y. Liu, J. Choi, Q. Sun, M. Elkashlan, and H. V. Poor, "Application of non-orthogonal multiple access in LTE and 5G networks," *IEEE Commun. Magazine*, vol. 55, no. 2, pp. 185-191, Feb. 2017.

[18] D. Nguyen, L. Tran, P. Pirinen, and M. Latva-aho, "Precoding for full duplex multiuser MIMO systems: Spectral and energy efficiency maximization," *IEEE Trans. Signal Process.*, vol. 61, no. 16, pp. 4038-4050, Aug. 2013.

[19] Y. Sun, D. W. K. Ng, Z. Ding and R. Schober, "Optimal joint power and subcarrier allocation for full-duplex multicarrier non-orthogonal multiple access systems," *IEEE Trans. Commun.*, vol. 65, no. 3, pp. 1077-1091, Mar. 2017

[20] Y. Sun, D. W. K. Ng, J. Zhu, and R. Schober, "Robust and secure resource allocation for full-duplex MISO multicarrier NOMA systems," *IEEE Trans. Commun.*, vol. 66, no. 9, pp. 4119-4137, Sept. 2018.

[21] Y. Zhang, H.-M. Wang, T.-X. Zheng, and Q. Yang, "Energy-efficient transmission design in non-orthogonal multiple access," *IEEE Commun. Surveys Tuts.*, vol. 66, no. 3, pp. 2852-2857, Mar. 2017.

[22] Y. Jing and H. Jafarkhani, "Single and multiple relay selection schemes and their achievable diversity orders," *IEEE Trans. Wireless Commun.*, vol. 8, no. 3, pp. 1414-1423, Mar. 2009.

[23] M. Gong, J. Zheng, and H. Chen, "Energy-efficient power allocation and user selection in amplify-and-forward relay networks," in *Proc. IEEE WCSP*, Yangzhou, Oct. 2016, pp. 1-5.

[24] M. Elsaadany and W. Hamouda, "Energy efficient design for non-orthogonal AF relaying in underlay spectrum sharing networks," in *Proc. IEEE ICC*, Kuala Lumpur, May 2016, pp. 1-6.

[25] Y. Hao, Y. Jing, and S. Panahi, "Energy efficient network beamforming design using power-normalized SNR," *IEEE Trans. Wireless Commun.*, vol. 13, no. 5, pp. 2756-2769, May 2014.

[26] Z. Han, D. Niyato, W. Saad, T. Basar, and A. Hjrungnes, "Game theory in wireless and communication networks: Theory, models, and applications," *Cambridge University Press, New York, NY, USA*, Jan. 2012.

[27] W. Dinkelbach, "On nonlinear fractional programming," *Management Science*, vol. 13, no. 7, pp. 492-498, Mar. 1967.

[28] H. Suzuki, T. V. A. Tran, I. B. Collings, G. Daniels, and M. Hedley, "Transmitter noise effect on the performance of a MIMO-OFDM hardware implementation achieving improved coverage," *IEEE J. Sel. Areas Commun.*, vol. 26, no. 6, pp. 867-876, Aug. 2008.

[29] W. Namgoong, "Modeling and analysis of nonlinearities and mismatches in AC-coupled direct-conversion receiver," *IEEE Trans. Wireless Commun.*, vol. 4, no. 1, pp. 163-173, Jan. 2005.

[30] H. Ju, E. Oh, and D. Hong, "Improving efficiency of resource usage in two-hop full duplex relay systems based on resource sharing and interference cancellation," *IEEE Trans. Wireless Commun.*, vol. 8, no. 8, pp. 3933-3938, Aug. 2009.

[31] Z. Zhang, Z. Ma, M. Xiao, Z. Ding, and P. Fan, "Full-duplex device-to-device-aided cooperative nonorthogonal multiple access," *IEEE Trans. Veh. Technol.*, vol. 66, no. 5, pp. 4467-4471, May 2017.

[32] G. Liu, X. Chen, Z. Ding, Z. Ma, and F. R. Yu, "Hybrid half-duplex/full-duplex cooperative non-orthogonal multiple access with transmit power adaptation," *IEEE Trans. Wireless Commun.*, vol. 17, no. 1, pp. 506-519, Jan. 2018.

[33] X. Yue, Y. Liu, S. Kang, A. Nallanathan, and Z. Ding, "Spatially random relay selection for full/half-duplex cooperative NOMA networks," *IEEE Trans. Commun.*, vol. 66, no. 8, pp. 3294-3308, Aug. 2018.

[34] K. Phan, S. Vorobyov, N. Sidiropoulos, and C. Tellambura, "Spectrum sharing in wireless networks via QoS-aware secondary multicast beamforming," *IEEE Trans. Signal Process.*, vol. 57, no. 6, pp. 2323-2335, Jun. 2009.

[35] B. P. Day, A. R. Margetts, D. W. Bliss, and P. Schniter, "Full-duplex MIMO relaying: Achievable rates under limited dynamic range," *IEEE J. Sel. Areas Commun.*, vol. 30, no. 8, pp. 1541-1553, Sep. 2012.

[36] Y. Choi and H. Shirani-Mehr, "Simultaneous transmission and reception: Algorithm, design and system level performance," *IEEE Trans. Wireless Commun.*, vol. 12, no. 12, pp. 5992-6010, Dec. 2013.

[37] S. Tombaz, A. Vastberg, and J. Zander, "Energy- and cost-efficient ultra-high-capacity wireless access," *IEEE Wireless Commun. Mag.*, vol. 18, no. 5, pp. 18-24, Oct. 2011.

[38] A. Mezghani and J. A. Nossek, "Power efficiency in communication systems from a circuit perspective," in *Proc. IEEE ISCAS*, Rio de Janeiro, Brazil , May 2011, pp. 1896-1899.

[39] D. Ray, "A game-theoretic perspective on coalition formation," *Oxford University Press*, 2007.

[40] A. Bogomolnaiaa and M. O.Jackson, "The stability of hedonic coalition structures," *Games and Economic Behavior*, vol. 38, no. 2, pp. 201-230, Feb. 2002.

[41] S. Boyd and L. Vandenberghe, "Convex optimization," Cambridge Univ. Press, 2004.

[42] 3GPP, TR 36.819 (V9.0.0), "Further advancement for E-UTRA physical layer aspects (Release 9)," Mar. 2010.

[43] M. Duarte, C. Dick, and A. Sabharwal, "Experiment-driven characterization of full-duplex wireless systems," *IEEE Trans. Wireless Commun.*, vol. 11, no. 12, pp. 4296-4307, Dec. 2012.

[44] Z. Yang, Z. Ding, P. Fan, and N. Al-Dhahir, "A general power allocation scheme to guarantee quality of service in downlink and uplink NOMA systems," *IEEE Trans. Wireless Commun.*, vol. 15, no. 11, pp. 7244-7257, Nov. 2016.

Keshav Singh (S'12, M'16) received the degree of Master of Technology in Computer Science from Devi Ahilya Vishwavidyalaya, Indore, India, in 2006, the M.Sc. in Information & Telecommunications Technologies from Athens Information Technology, Greece, in 2009, and the Ph.D. degree in Communication Engineering from National Central University, Taiwan, in 2015. In the past, he worked as a Research Associate at the University of Edinburgh, UK. Currently, he is currently working as a Research Scientist at the University College Dublin (UCD), Ireland. His current research interests are in the areas of Green Communications, Resource Allocation, Full-Duplex Radio, Green Networks, URLLC, Non-Orthogonal Multiple Access (NOMA), Wireless Edge Caching and Machine Learning for Communications.

Kaidi Wang (S'16) received the MS degree in communications and signal processing from Newcastle University, UK, in 2014. He is currently working toward the PhD degree in wireless communication with the University of Manchester, UK. He was with Lancaster University from 2015 to 2018. His current research interests include game theory, convex optimization, non-orthogonal multiple access, and 5G wireless networks.

Sudip Biswas (S'16, M'17) received the B.Tech. degree in Electronics and Communication Engineering from Sikkim Manipal Institute of Technology, Sikkim, India, in 2010, the M.Sc. degree in Signal Processing and Communications from the University of Edinburgh, Edinburgh,U.K., in 2013, and the Ph.D. degree in Digital Communications from the University of Edinburgh's Institute for Digital Communications (IDCOM) in 2017. Currently, he is working as a Research Scientist in IDCOM, University of Edinburgh. His research interests include various topics in wireless communications and network information theory with particular focus on possible 5G technologies such as Massive Multiple-Input and Multiple-Output (MIMO), mmWave, Full-Duplex Radio, Wireless Caching, Non-Orthogonal Multiple-Access, and Machine Learning for Communications.

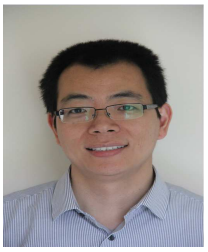

Zhiguo Ding received his Ph.D from Imperial College London in 2005. He is currently a Professor in Communications at the University of Manchester. From Sept. 2012 to Sept. 2019, he has also been an academic visitor in Princeton University. Dr Ding' research interests are 5G networks, game theory, cooperative and energy harvesting networks and statistical signal processing. He has been serving as an Editor for IEEE TCOM, IEEE TVT, and served as an editor for IEEE WCL and IEEE CL. He received the best paper award in ICWMC-2009 and WCSP-2015, IEEE Communication Letter Exemplary Reviewer 2012, the EU Marie Curie Fellowship 2012-2014, IEEE TVT Top Editor 2017, 2018 IEEE Communication Society Heinrich Hertz Award, 2018 IEEE Vehicular Technology Society Jack Neubauer Memorial Award, and 2018 IEEE Signal Processing Society Best Signal Processing Letter Award.

Faheem A. Khan (M'02) is currently a Senior Lecturer with the School of Computing and Engineering, University of Huddersfield, U.K. He received the Ph.D. degree in electrical and electronic engineering from Queens University Belfast, U.K., in 2012. In the past, he worked as a Postdoctroral Research Associate with the Institute for Digital Communications, University of Edinburgh, U.K., where he contributed to research in EU research projects HARP and ADEL. He has authored or coauthored more than 20 papers in refereed journals and conferences. His research interests include the field of wireless communications and signal processing with particular focus on cognitive radio, MIMO, and millimeter-wave communications. He has significant previous teaching and research experience at academic institutions in the U.K., Middle East, and India. He is a Fellow of the Higher Education Academy, U.K.

Tharmalingam Ratnarajah (A'96-M'05-SM'05) is currently with the Institute for Digital Communications, University of Edinburgh, Edinburgh, UK, as a Professor in Digital Communications and Signal Processing. His research interests include signal processing and information theoretic aspects of 5G and beyond wireless networks, full-duplex radio, mmWave communications, random matrices theory, interference alignment, statistical and array signal processing and quantum information theory. He has published over 330 publications in these areas and holds four U.S. patents. He was the coordinator of the FP7 projects ADEL (3.7M€) in the area of licensed shared access for 5G wireless networks and HARP (4.6M€) in the area of highly distributed MIMO and FP7 Future and Emerging Technologies projects HIATUS (3.6M€) in the area of interference alignment and CROWN (3.4M€) in the area of cognitive radio networks. Dr Ratnarajah is a Fellow of Higher Education Academy (FHEA), U.K..